Journal of Energy Storage 27 (2020) 101125

Contents lists available at ScienceDirect

Journal of Energy Storage

journal homepage: www.elsevier.com/locate/est

Corrosion evaluation of eutectic chloride molten salt for new generation of CSP plants. Part 1: Thermal treatment assessment

Angel G. Fernández*, Luisa F. Cabeza

GREiA Research Group, INSPIRES Research Centre, Universitat de Lleida, Pere de Cabrera s/n, 25001 Lleida, Spain

ARTICLE INFO

Keywords:
Concentrated solar power
Thermal energy storage
Corrosion mitigation
Chloride molten salt
Thermal purification treatment

ABSTRACT

The operating temperature of a steam turbine is limited to 565 ºC by the molten nitrate heat-transfer fluid; therefore, a new molten salt chemistry is needed to increase the maximum operating temperature in the new generation of CSP plants and improve the thermal-to-electrical energy conversion efficiency in the turbine block, such as chloride molten salts. Nevertheless, the prevention of high-temperature corrosion on containment materials using chlorides plays a critical role and a corrosion mitigation plan is needed to achieve the target plant lifetime of 30 years. This paper presents a corrosion mitigation strategy focused on different thermal treatments performed in the eutectic ternary chloride molten salt composed by $MgCl_2$/NaCl/KCl (55.1 wt.%/24.5 wt.%/20.4 wt.%). Corrosion rates were obtained through linear polarization resistance technique in a conventional commercial stainless steel (AISI 304) at 720 ºC during 5 h of immersion after the different thermal treatments carried out. Scanning electron microscopy and XRD analysis were used to confirm the corrosion rates and corrosion layer proposed by electrochemical techniques, obtaining a minimum corrosion rate of 6.033 mm/year for the best thermal treatment performed.

1. Introduction

During the last years the cost of CSP technology was reduced, but an additional effort is necessary to compete with other renewables technologies as PV. On average, the projected cost for a CSP plant dropped by about 9 ¢USD/kWh cents per kilowatt hour, from 21 ¢USD/kWh in 2010 to 12 ¢USD/kWh in 2015 and anticipated to reach 10 ¢USD/kWh in 2017 [1]. To continue these cost reductions in solar technologies, US department of energy (DOE) recently established cost targets for 2030 that would make to this renewable energy, one of the lowest-cost sources of electricity provided by CSP technology. The new targets correspond to a levelized cost of electricity (LCOE) in 2030 of $0.05/kWh for a dispatchable, high-capacity factor CSP-TES plant configuration [2]. Past and future cost reductions of CSP are tied to improve system wide performance. Particularly, increasing the maximum operating temperature and thereby the thermal to electric conversion efficiency reduces the required capacity of the entire plant strongly influencing cost reduction.

The selection of a high-temperature molten-salt chemistry is needed, as well as the need to understand its impact on containment materials, to achieve acceptable strength, durability, and cost targets at these high temperatures [3]. Table 1 shows the molten salt candidates that were analyzed in this direction.

Carbonates and fluoride salts need to include lithium in their formulations in order to reduce their melting points to levels below 500ºC, increasing the final cost for the thermal energy storage material [5]. On the other hand, chloride molten salts are considered a feasible option due to their low cost and high decomposition temperature [6].

One of the most studied mixtures is composed by $MgCl_2$/NaCl/KCl (55.1 wt.%/24.5 wt.%/20.4 wt.%) since it has a melting point of 380 ˚C, thermal stability up to 800 ˚C, higher heat capacity compared to chloride salts containing $ZnCl_2$, and low vapor pressure [4]. This last parameter is one of the main drawback using $ZnCl_2$ due to their important increase at 530 ˚C [3]. But these molten salts introduce a set of technological and engineering challenges because of their very corrosive nature on typical containment materials. Corrosion mitigation approaches were investigated trying to achieve a corrosion rate around 20 μm/year or lower for the containment materials, thus providing a plant lifetime of 30 years or longer [7,8]. Nevertheless, this scope is still far and corrosion mitigation strategies are needed to reduce corrosion to these levels. One of these strategies is the performance of thermal purification treatments before corrosion tests using chloride molten salts.

The aim of this paper is to analyze different thermal purification treatments to reduce corrosive impurities and hence corrosion rates obtained in a conventional austenitic stainless steel (AISI 304)

* Corresponding author.
E-mail address: angel.fernandez@diei.udl.cat (A.G. Fernández).

https://doi.org/10.1016/j.est.2019.101125
Received 2 August 2019; Received in revised form 4 November 2019; Accepted 30 November 2019

Table 1
Molten salts proposed for high temperature TES [3].

Molten salt composition (wt.%)	Melting point (ºC)	Thermal stability limit (ºC)	Density (g/cm^3)	Heat capacity (kJ/kg* K)	Material cost (USD/kg)
60$NaNO_3$/40KNO_3	223	565	1.8 (400ºC)	1.5 (400ºC)	0.8
32 K_2CO_3 + 35 Li_2CO_3 + 33 Na_2CO_3	397	>650	2.0 (700ºC)	1.9 (700ºC)	2.5
59 KF + 29 LiF +12 NaF	454	>700	2.0 (700ºC)	1.9 (700ºC)	>2
23.9 KCl + 7.5 NaCl + 68.6 $ZnCl_2$	204	850	2 (600ºC)	0.8 (300–600ºC)	0.8
20.4 KCl + 55.1 $MgCl_2$ + 24.5 NaCl	380	800	1.7 (600ºC)	1.0 (500–800ºC)	<0.35

Table 2
Chemical composition of ternary chloride salt tested.

K (%)	Mg (%)	Na (%)	Mn (ppm)	SO_4 (ppm)	Cl (%)	H_2O (%)
20.6	11.9	3.4	1.8	162	60	5

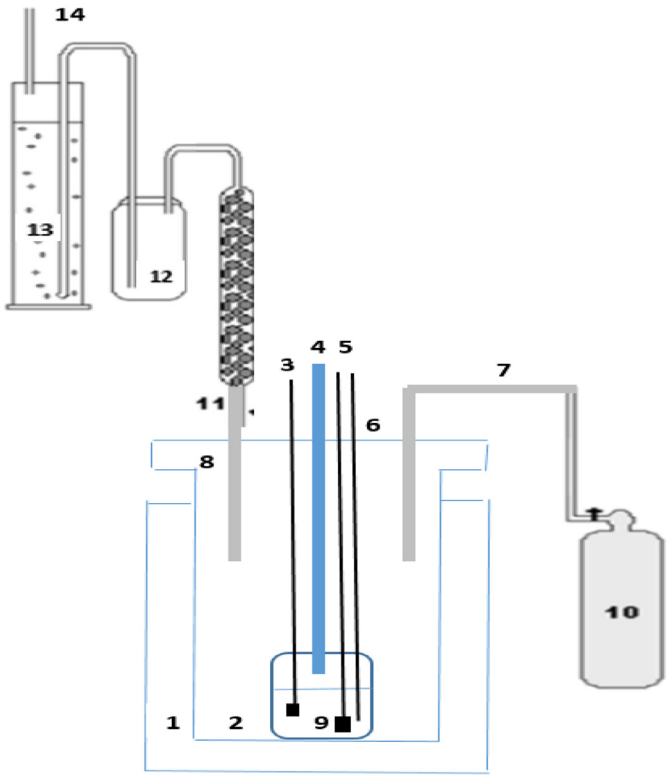

Fig 1. Experimental setup of electrochemical test in controlled atmosphere: 1: furnace; 2: molten salt reactor; 3: counter electrode, 4: thermocouple, 5: working electrode, 6: reference electrode, 7: gas inlet, 9: molten salt, 10: carrier gas, 8: off-gas system (which consists of 11: MgO trap for chlorine; 12: moisture removal; 13: 1 M NaOH scrubber; and 14: gas exhaust).

immersed in the ternary $MgCl_2$/NaCl/KCl (55.1 wt.%/24.5 wt.%/20.4 wt.%) molten salt during 5 h at 720 °C using linear polarization resistance technique.

2. *Corrosive impurities present in chloride molten salts*

Corrosion in molten chlorides is driven by the impurities in the salt, such as H_2O, OH^-, O_2, and H^+ since it can destabilize passive surface oxide films [9,10]. One of the main important impurities present in molten chlorides, especially in $MgCl_2$, are hydroxychlorides [11]. Hydroxychlorides are formed via hydrolysis when $MgCl_2$ is dried such that the chlorides with hydrated H_2O molecules form hydroxychloride and HCl gas at high temperature [12,13,14]. At higher temperatures, the hydroxychloride partially decomposes to its corresponding oxide and HCl gas [15,16] while the undecomposed portion dissociates to form OH^-, which can remain in the molten chloride.

Although no solubility of MgOHCl in molten $MgCl_2$ was reported, its dissolution in molten $MgCl_2$-containing salts is believed to involve the formation of complex molecules between Mg^{2+} ion and $MgOH^+$ ion [17] or a dimer structure with two MgOHCl molecules. Vilnyansky and Bakina [18], confirmed that MgO is practically insoluble in $MgCl_2$—NaCl and Ozeryanaya et al. [19] reported that oxygen (Ks = 10^{-8} mol/cm^3), chlorine (Ks = (0.03–4.62) $\times 10^{-6}$ mol/cm^3), and hydrogen chloride (Ks = (0.19–3.16) $\times$ 10^{-6} mol/cm^3) possess a low solubility Ks in molten alkali and alkaline-earth chlorides at temperatures between 650 °C and 950 °C. However, the oxidizing gases dissolved in molten chlorides cause corrosion and Fe^{2+}, Cr^{2+} and Ni^{2+} ions can form low solubility oxides with oxygen ions in the molten salt.

Additionally, Grabke et al. [20] analyzed the presence of SO_2 in chloride molten salt and concluded that it causes a minor increase of active corrosion by sulfation of chlorides and generation of chlorine. According to this, one of the key efforts in molten chloride corrosion mitigation has focused on reducing the corrosive impurities by suppressing the side reactions of hydrolysis during salt heating [4]. In the molten salt proposed, $MgCl_2$ (from raw material) is in the form of hexahydrate, and some authors [4,21] identified the formation of MgOHCl through the following reaction at 167 °C [21]:

$$MgCl_2.2H_2O \grave{a} MgOHCl + HCl + H_2O$$

The dehydration of the monohydrate occurs at 235 °C and also produces MgOHCl:

$$MgCl_2.\ H_2O \cdot \rightarrow \cdot \grave{a} MgOHCl + HCl$$

Thermal decomposition of MgOHCl was reported to occur between 415 °C and 555 °C [21,22], which produces MgO and HCl:

$$MgOHCl \rightarrow \cdot \grave{a} MgO + HCl$$

3. Experimental procedures

The molten salt tested was the eutectic mixture 20.4 KCl + 55.1 $MgCl_2$ + 24.5 NaCl (Sigma Aldrich 99%) at 720 °C under inert atmosphere (N_2). Some analysis were carried out in the commercial salts used in this research (Table 2):

A two electrodes arrangement was used, composed by a working electrode (WE) and reference-counter (RE-CE) electrodes, that were immersed in the molten salt (electrolyte), and the open circuit potential (OCP) was measured using a potentiostat (Gamry 1010E). The experimental set up is shown in Fig. 1.

It is necessary to purify and refresh the gas release from the reactor (2). For this purpose, a MgO trap (11) is included to remove water content and a NaOH trap (13) to neutralize H^+ that could be produce during the experiments. Linear polarization tests were carried out from a potential of −0.6 V to 0.4 V of the OCP voltage using a scanning range of 0.005 V/s with steps of 0.00244 V. A specific thermal treatment during the melting process must be defined in order to reduce the corrosive impurities present in commercial chloride molten salts, especially in $MgCl_2$. The easiest way to prevent the contamination of O_2 and H_2O is to thoroughly dry the hygroscopic $MgCl_2$ salt. The temperatures at each drying stage were determined from the vapor–-pressure curves in Fig. 2.

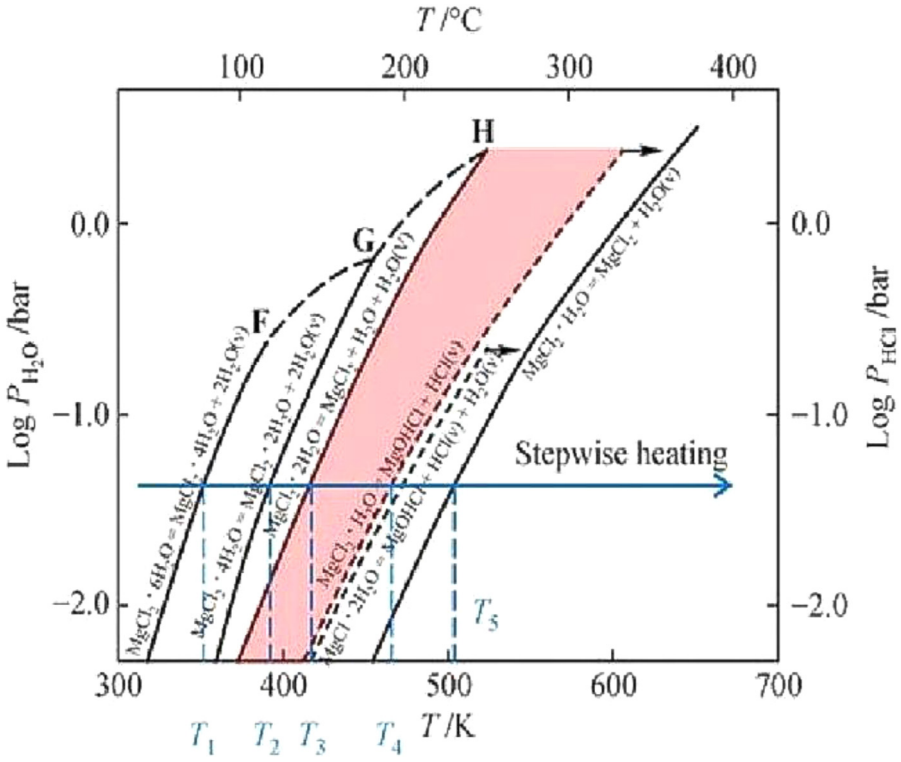

Fig 2. Vapour pressure of H_2O and HCl curve on $MgCl_2$•$7H_2O$.

Table 3
Specific conditions for thermal treatments in ternary chloride molten salt.

Thermal treatment	Temperature (°C)	Dwelling time (h)	Reference
1	117	16	[25]
	180	8	
	240	16	
	300	1	
	450	1	
	600	1	
	720	–	
2	70	2	Proposed in this study
	117	2	
	145	4	
	190	4	
	227	4	
	300	4	
	450	3	
	600	1	
	720	–	
3	200 (Heating ramp: 5°C/min)	1	[23]
	700	–	
4	70	0.5	Proposed in this study
	117	0.5	
	145	0.5	
	190	0.75	
	227	0.75	
	300	0.25	
	450	0.25	
	600	0.25	
	720	–	

Some authors [23–25] proposed a multi-step heating to purify $MgCl_2$ salts and to reduce the formation of MgOHCl. In this research we have analyzed different thermal treatments, at different dwelling times at each temperature, to compare those available in the literature as well as new ones proposed in this study, with a more specific stepwise heating at T1-T5 shown in Fig. 2. Specific conditions for thermal treatments performed are shown in Table 3.

Table 4
Chemical composition of stainless steel AISI 304.

Stainless Steel	wt.% Si	Mn	Cr	P	C	S	Ni	Fe
304	0.75	2	18	0.045	0.08	0.03	8	Balance

Vidal and Klammer [26] stablished different key temperatures (treatment #1) using long dwelling times for each temperature, but heating ramps were not reported. On the other hand, Ding et al. [23] stablished a quick thermal treatment only using a heating step at 200 °C, using a heating ramp of 5 °C/min. After this step, no heating ramps or additional temperature steps were reported before reaching the testing temperature (700 °C).

Additionally, other two heat treatments (#2 and #4) were carried out, following a more specific stepwise heating through $MgCl_2$ water molecules release and using a heating ramp of 10 °C/min, according to Fig. 2. In the last thermal treatment proposed (#4), dwelling times were reduced compared to thermal treatment #2.

The salts were carefully handled and mixed to avoid water absorption in a dry box containing desiccants and after the thermal purification treatment the salt was solidified and the bottom part was removed, with the insoluble impurities.

The corrosion behavior after thermal treatments was evaluated in the same alloy, AISI 304, with a chemical composition shown in Table 4.

Corrosion evaluation assessment were carried out using linear polarization resistance technique. To quantify the polarization resistance R_p, it is important to take into account the potential drop attributed to the electrolyte resistance (molten salts). The relationship between polarization resistance and corrosion current density i_{corr}, is given by Eq. (1):

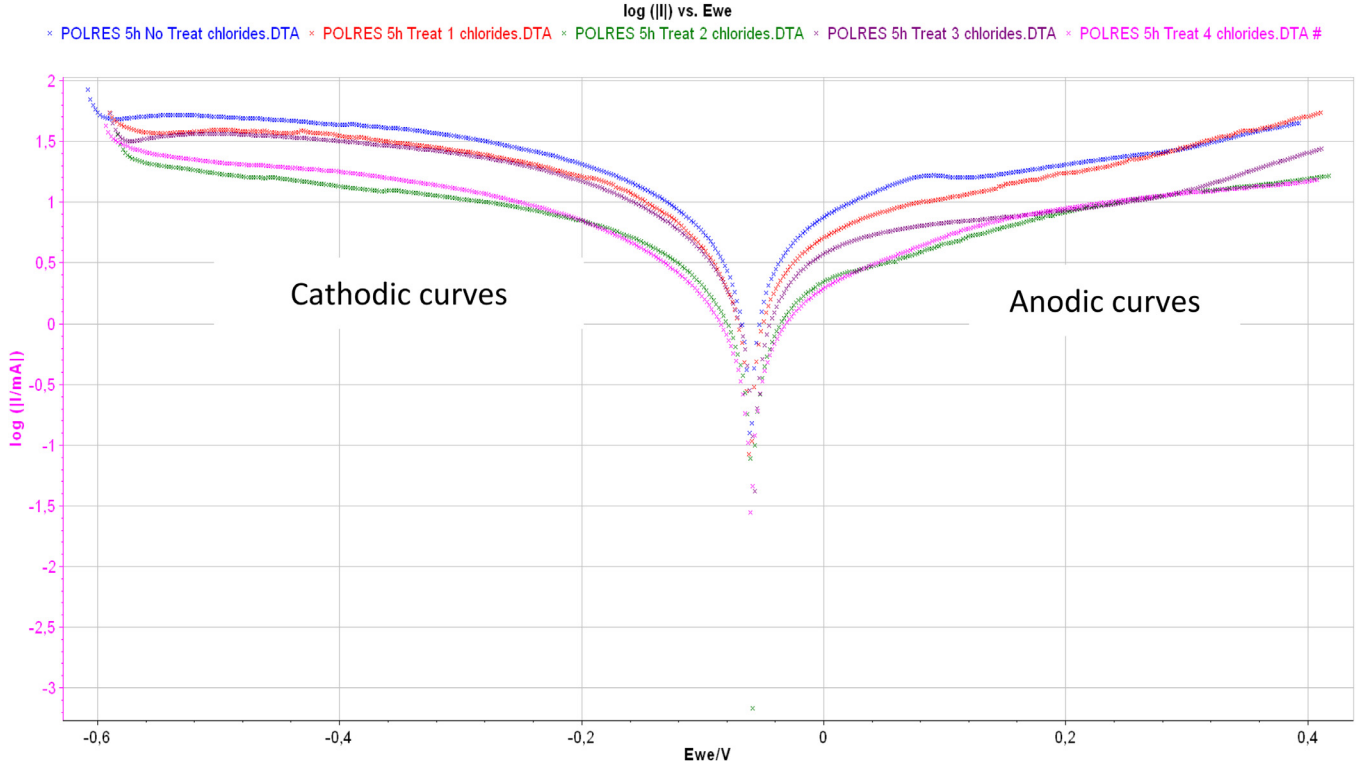

Fig 3. Linear polarization curves for the different thermal treatments performed in AISI304 after 5 h of immersion in the ternary chloride molten salt.

Table 5
Corrosion parameters obtained for AISI304 immersed in chloride molten salt during 5 h at 720 °C after different thermal treatments .

Steel	Thermal treatment	E_{corr} (mV)	j_{corr} (mA)	CR (mm/year)	β_α (V/dec)	β_c (V/dec)
304	No treatment	−61.506	11.926	19.66	1.230	0.525
304	1	−58.166	9.688	12.559	0.798	0.427
304	2	−58.745	2.929	6.033	0.572	0.379
304	3	−59.071	4.985	10.627	0.960	0.598
304	4	−61.112	5.097	9.935	0.494	0.271

$$i_{corr} = \frac{B}{R_p} \quad (1)$$

where B is an electrochemical constant calculated theoretically according to the Eq. (2):

$$B = \frac{\beta_\alpha \cdot n\beta_c}{2,3 \cdot n(\beta_\alpha + \beta_c)} \quad (2)$$

where β_c and β_α are the cathodic and anodic Tafel slope, respectively.

The B parameter must be used to convert the R_p values into corrosion current densities, so it is necessary to make a derivation of the polarization curves according to Eq. (3):

$$R_p = \left.\frac{\Delta E}{\Delta i}\right|_{E=E_{corr}} = \frac{B}{i_{corr}} = \frac{\beta_\alpha \cdot \beta_c}{i_{corr} \cdot 2,3 \cdot (\beta_\alpha + \beta_c)} \quad (3)$$

The corrosion density current i_{corr} and the corrosion potential E_{corr} were determined from the extrapolation of the Tafel curve.

The corrosion rate (CR) can be estimated through the Butler-Volmer equation showed in Eq. (4):

$$CR = \frac{i_{corr} \cdot K}{\rho_{alloy} \cdot \sum \left(\frac{f_i \cdot n_i}{MW_i}\right)} \quad (4)$$

where K is a correlation constant that defines the units of CR (3272 for CR in mm/year), ρ_{alloy} is the alloy density (g/cm^3), f_i is the mole fraction of the element i in the alloy, n_i is the number of electrons that are transferred in element i and MW_i is the atomic weight of element i.

Finally, after the corrosion test, the metal specimens were analyzed by scanning electron microscopy (SEM) and x-ray diffraction (XRD) to detect the corrosion produced. The XRD device used was the PANalytical X´Pert PRO model, and measures were taken from 5 to 120° with a step size of 0.017°, while the SEM model used was the Quanta 250, Thermofisher.

4. Results and discussions

The different thermal treatments were carefully addressed before reaching the testing temperature (720 °C). After that, linear polarization technique was carried out after 5 h of immersion of AISI 304 in the ternary $MgCl_2$/NaCl/KCl (55.1 wt.%/24.5 wt.%/20.4 wt.%) molten salt. All Tafel curves for the different experiments carried out in this study are shown Fig. 3.

The corrosion rate results obtained from Fig. 3, according to Eq. (4), are shown in Table 5.

As expected, the highest corrosion rate was obtained in the steel without a previous thermal treatment in the salt, followed by Treat #1 > 3 > 4 > 2. The lowest corrosion rate was obtained in thermal treatment #2, which corresponds to the more specific stepwise heating (Table 1) proposed in this study.

These results were confirmed by scanning electron microscopy (SEM). Fig. 4 shows the superficial top-view (left) and cross-sectional image (right) for the different thermal treatment performed in the chloride salt, after immersion in chloride molten salt during 5 h at 720 °C. Results also include an energy dispersive x-ray analysis (EDX) in the corrosion layer found in the cross sectional study.

Micrographs are in concordance with corrosion rate values obtained by linear polarization resistance technique (Table 3). The sample without thermal treatment (Fig. 4a) showed the highest corrosion

a) No thermal treatment

Analysis	O	Mg	Cl	K	Fe
A (wt.%)	14.86	5.75	61.77	10.46	7.16

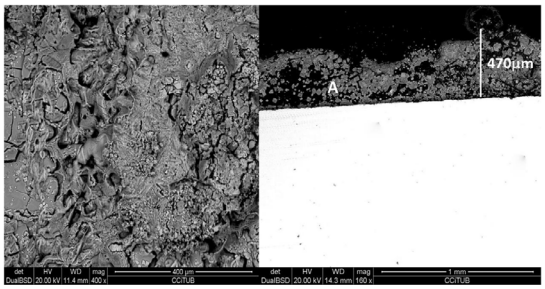

b) Thermal treatment #1

Analysis	O	Na	Cl	K	Fe
A (wt.%)	13.51	3.06	49.82	33.62	3.46

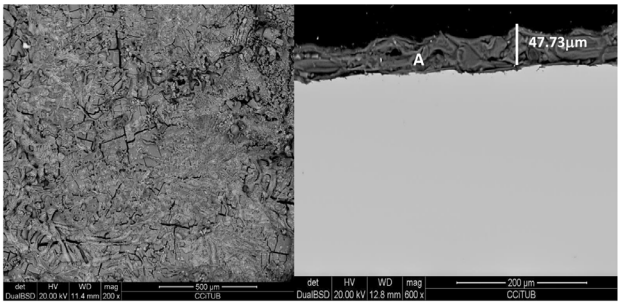

c) Thermal treatment #2

Analysis	O	Mg	Cl	Cr	Fe
A (wt.%)	21.50	46.63	7.92	9.91	14.53

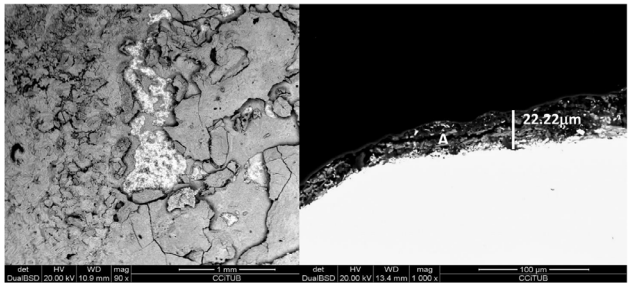

d) Thermal treatment #3

Analysis	O	Mg	Cl	Cr	Fe
A (wt.%)	10.65	9.63	13.51	7.59	58.62

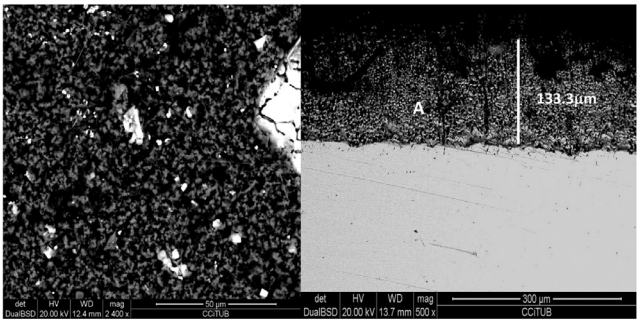

e) Thermal treatment #4

Analysis	O	Mg	Cl	Cr	Fe
A (wt.%)	11.55	35.74	3.52	5.93	43.26

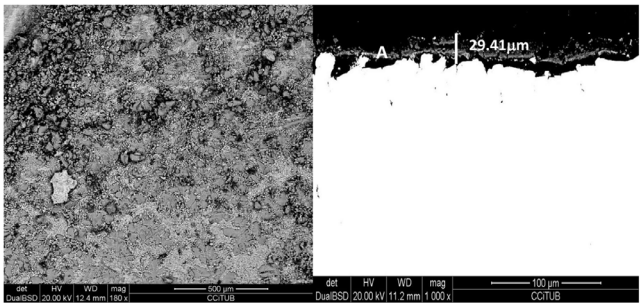

Fig 4. Superficial (left) and cross sectional (right) study for AISI304 immersed in $MgCl_2$/NaCl/KCl (55.1 wt.%/24.5 wt.%/20.4 wt.%) during 5 h following (a) No thermal treatment, (b) thermal treatment #1, (c) thermal treatment #2, (d) thermal treatment #3, and (e) thermal treatment #4.

average layer thickness (470 µm) with potassium, chloride and oxygen as main components. XRD analysis (Table 5) confirmed the compounds detected in this layer and MgOHCl, MgO and KCl were obtained. It is important to highlight that MgOHCl was pointed in the literature as one of the most corrosive impurities present in chloride salts [4,23, 24, 25]. In the following tests with the different thermal treatments performed (Fig. 4b–e) before the corrosion test, this compound was reduced, obtaining lower content in chloride from the EDX carried out in the steel surface. The lowest corrosion layer thickness corresponds to thermal treatment #2 (22.22 µm) in concordance with corrosion rates obtained by linear polarization resistance (LPR) (Table 5). This treatment was developed following a more specific stepwise heating according to vapor pressure curve on $MgCl_2$•$7H_2O$.

EDX analysis carried out in the steel surface showed the elements detected in the corrosion layer. Chromium content was detected in the protective layer of thermal treatment #2, #3 and #4 but it is important to highlight that the diffusion coefficient in Cr is lower compared to Fe. Additionally, an uniform corrosion mechanism was observed in the micrographs shown in Fig. 4.

In order to complete the corrosion characterization in the stainless steel tested, XRD analysis were performed in the stainless steels. Fig. 5 shows the XRD obtained in AISI 304 after the corrosion test in $MgCl_2$/NaCl/KCl (55.1 wt.%/24.5 wt.%/20.4 wt.%) with thermal treatment #2.

In this case, a protective layer composed by $MgCr_2O_4$ was detected as well as magnetite (Fe_3O_4) and MgO as the main corrosive compounds formed in the steel surface. All the XRD results obtained in the alloys immersed in chloride molten salts along with the different thermal treatment performed are shown in Table 6.

In this case, corrosion products containing magnesium, chloride and oxygen were detected in the experiments with thermal treatments that corresponds to higher corrosion rates. In this direction, corrosion test without a previous purification treatment showed the presence of MgOHCl, as the main aggressive impurity present in chloride molten salts.

5. Conclusions

A specific purification treatment is necessary to reduce the corrosive impurities in chloride molten salts to be used in the new generation of

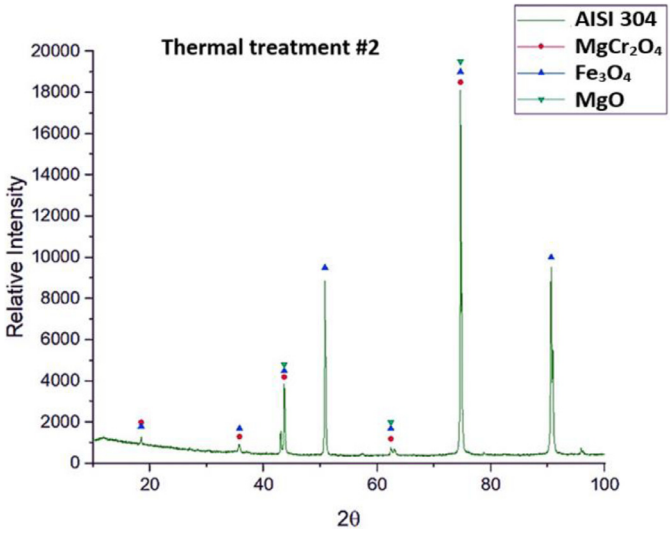

Fig 5. XRD analysis obtained in AISI 304 stainless steel after 5 h of immersion in $MgCl_2$/NaCl/KCl (55.1 wt.%/24.5 wt.%/20.4 wt.%) during 5 h at 720 °C.

Table 6
Corrosion products identified by XRD analysis on AISI304 after exposure to the salt mixture at 720 °C for 5 h.

Salt mixture	Thermal Treatment	Corrosion Products	Reference Pattern
$MgCl_2$/NaCl/KCl (55.1wt.%/24.5wt.%/20.4wt.%)	No treatment	MgOHCl	00-012-0120
		MgO	01-087-0651
		KCl	01-072-1540
	1	MgO	01-087-0651
		NaCl	01-077-2064
		Fe_3O_4	01-086-1353
	2	$MgCr_2O_4$	01-082-1529
		MgO	01-087-0651
		Fe_3O_4	01-086-1353
	3	KCl	00-004-0587
		Fe_3O_4	01-086-1353
		$FeCr_2O_4$	00-024-0511
	4	MgO	01-087-0651
		$MgFe_2O_4$	01-073-1960
		$MgCl_2$	00-003-0854
		$FeCr_2O_4$	00-024-0511

CSP plants. Corrosion in molten chlorides is driven by the impurities in the salt, H_2O, OH^-, O_2, and H^+. The formation of MgOHCl was identified as the most important corrosive impurity, and a specific thermal treatment at $MgCl_2$ water removement temperatures needs to be developed before corrosion tests.

A viable method for drying and purifying chloride salts is proposed in this paper. The thermal treatment selected could be applied in the commercial application in a cost effective way minimizing times involved for drying/heating energy requirements.

An important corrosion rate reduction was obtained after thermal treatment selected in this research, reducing this parameter 68%, from 19.66 mm/year to 6.33 mm/year.

Declaration of Competing Interest

The authors declare that they have no known competing financial interests or personal relationships that could have appeared to influence the work reported in this paper.

Acknowledgments

Angel G. Fernández wants to acknowledge the financial support from the European Union's Horizon 2020 research and innovation programme under the Marie Sklodowska-Curie grant No 712949 (TECNIOspring PLUS) and from the Agency for Business Competitiveness of the Government of Catalonia. This work was partially funded by the Ministerio de Ciencia, Innovación y Universidades de España (RTI2018-093849-B-C31). The authors would like to thank the Catalan Government for the quality accreditation given to their research group GREiA (2017 SGR 1537). GREiA is a certified agent TECNIO in the category of technology developers from the Government of Catalonia. This work is partially supported by ICREA under the ICREA Academia programme.

Supplementary materials

Supplementary material associated with this article can be found, in the online version, at doi:10.1016/j.est.2019.101125.

References

[1] IEA, Concentrating Solar Power Roadmap. http://www.iea.org/publications/freepublications/publication/csp_roadmap.pdf, 2010.
[2] Caitlin Murphy, Y.S, Wesley Cole, Galen Maclaurin, Craig Turchi, Mark Mehos, The Potential Role of Concentrating Solar Power Within the Context of Doe's 2030 Solar Cost Targets, (2019), pp. 6A20–71912 NREL/TP.
[3] M. Mehos, C.T.J. Vidal, M. Wagner, Z. Ma, C. Ho, W. Kolb, C. Andraka, A. Kruizenga, Concentrating Solar Power Gen3 Demonstration Roadmap, (2017), pp. 5500–67464. Technical ReportNREL/TP.
[4] W. Ding, A. Bonk, T. Bauer, Corrosion behavior of metallic alloys in molten chloride salts for thermal energy storage in concentrated solar power plants: a review, Front. Chem. Sci. Eng. 12 (2018) 564–576.
[5] K. Vignarooban, Vapor pressure and corrosivity of ternary metal-chloride molten-salt based heat transfer fluids for use in concentrating solar power systems, Appl. Energy 159 (2015) 206–213.
[6] A.M. Kruizenga, Corrosion Mechanisms in Chloride and Carbonate Salts (2012) 2012–7594 Sandia Report, SAND.
[7] J.C. Gomez-Vidal, A.G. Fernandez, R. Tirawat, C. Turchi, W. Huddleston, Corrosion resistance of alumina-forming alloys against molten chlorides for energy production. I: pre-oxidation treatment and isothermal corrosion tests, Solar Energy Mater. Solar Cells 166 (2017) 222–233.
[8] J.C. Gomez-Vidal, A.G. Fernandez, R. Tirawat, C. Turchi, W. Huddleston, Corrosion resistance of alumina forming alloys against molten chlorides for energy production. II: electrochemical impedance spectroscopy under thermal cycling conditions, Solar Energy Mater. Solar Cells 166 (2017) 234–245.
[9] X.K. Feng, C.M. Melandres, Anodic corrosion and passivation behavior of some metals in molten LiCl-KCl containing oxide ions, J. Electrochem. Sci. Technol. 129 (1982) 1245–1249.
[10] Y.P. Zaikov, V.P. Batukhtin, N.I. Shurov, L.E. Ivanovskii, A.V. Suzdaltsev, "Calcium production by the electrolysis of molten $CaCl_2$ - part I. interaction of calcium and copper-calcium alloy with electrolyte," metall. Mater. Trans. B Process Metall, Mater. Process. Sci 45 (2014) 961–967.
[11] H.-.C. Eom, H. Park, H.-.S. Yoon, Preparation of anhydrous magnesium chloride from magnesium chloride hexahydrate, Adv. Power Technol. 21 (2010) 125–130.
[12] Q. Huang, G. Lu, J. Wang, J. Yu, Thermal decomposition mechanisms of $MgCl_2$•$6H_2o$ and $MgCl_2$•H_2o, J. Anal. Appl. Pyrolysis 91 (2011) 159–164.
[13] S. Kashani-Nejad, Oxides in the Dehydration of Magnesium Chloride Hexahydrate, McGill University, 2005.
[14] S. Kashani-Nejad, K.W. Ng, R. Harris, Preparation of MgOHCl by Controlled Dehydration of $MgCl_2$ $6H_2O$, Metall. Mater. Trans. B 35 (2) (2004) 405–406.
[15] S. Kashani-Nejad, K.W. Ng, R. Harris, Properties of MgOHCl, Metall. Mater. Trans. B. 35 (2004) 406–408.
[16] J. de Bakker, J. Peacey, B. Davis, Thermal decomposition studies on magnesium hydroxychlorides, Can. Metall. Q. 51 (2012) 419–423.
[17] S. Kashani-Nejad, K.W. Ng, R. Harris, "MgOHCl thermal decomposition kinetics," Metall. Mater. Trans. B Process Metall. Mater. Process. Sci. 36 (2005) 153–157.
[18] J.E. Vindstad, H. Mediaas, T. Ostvold, Hydrolysis of $MgCl_2$-containing melts, Acta Chem. Scand. 51 (1997) 1192–1200.
[19] Y.E. Vilnyansky, N.P. Bakina, Solubility of water and magnesium oxide in fused carnallite, J. Appl. Chem. USSR. 29 (1956) 615–619.
[20] I.N. Ozeryanaya, Corrosion of metals by molten salts in heat-treatment processes, Metal Sci. Heat Treat. 27 (1985) 184–188.
[21] H.J. Grabke, E. Reese, M. Spiegel, The effects of chlorides, hydrogen chloride, and sulphur dioxide in the oxidation of steels below deposits, Corros Sci. (1995) 1023–1043.
[22] Q. Huang, G. Lu, J. Wang, J. Yu, Thermal decomposition mechanisms of $MgCl_2$•$6H_2o$ and $MgCl_2$•H_2o, J. Anal. Appl. Pyrolysis 91 (2011) 159–164.
[23] G.J. Kipouros, D.R. Sadoway, The chemistry and electrochemistry of magnesium production, in: G. Mamantov, C.B. Maman- tov, J. Braunstein (Eds.), The chemistry and electrochemistry of magnesium production, Adv. Molten Salt Chem. 6 (1987) 127–209.
[24] W. Ding, H. Shi, Y. Xiu, A. Bonk, A. Weisenburger, A. Jianu, T. Bauer, Hot corrosion

behavior of commercial alloys in thermal energy storage material of molten $MgCl_2$/KCL/NaCl under inert atmosphere, Solar Energy Mater. Solar Cells 184 (2018) 22–30.

[25] H.Shi W.Ding, A. Jianu, A. Bonk, A. Weisenburger, T. Bauer, Molten chloride salts for next generation concentrated solar power plants: mitigation strategies against corrosion of structural materials, Solar Energy Mater. Solar Cells 196 (2019) 298–313.

[26] J. Vidal, N. Klammer, Molten chloride technology pathway to meet the U.S, DOE SunShot Initiative with Gen3 CSP. SolarPACES conference, Casablanca, Morocco, 2018.